

From the Department of Clinical Science, Intervention and Technology  
(CLINTEC), Division of Radiography,  
Karolinska Institutet, Stockholm, Sweden

# **PET/CT WITH 18F-FDG AND 68GA- DOTATOC IN PULMONARY CARCINOID IMAGING**

Natalja Uhlén



**Karolinska  
Institutet**

Stockholm 2019

All previously published papers were reproduced with permission from the publisher.

Published by Karolinska Institutet.

Printed by AJ E-print AB

© Natalja Uhlén, 2019

ISBN 978-91-7831-550-5

# PET/CT with 18F-FDG and 68Ga-DOTATOC in pulmonary carcinoid imaging

## THESIS FOR LICENTIATE DEGREE

By

**Natalja Uhlén**

*Principal Supervisor:*

Professor Rimma Axelsson  
Karolinska Institutet  
Department of Clinical Science,  
Intervention and Technology  
Division of Radiology

*Co-supervisor(s):*

Professor Anders Sundin  
Uppsala University  
Department of Surgical Sciences

Doctor Karl-Gustaf Kölbeck  
Karolinska Institutet  
Department of Medicine  
Division of Respiratory Medicine

*Examination Board:*

Docent Maria Kristoffersen Wiberg  
Karolinska Institutet  
Department of Clinical Neuroscience

Docent Elin Trägårdh  
Lund University  
Department of Translational Medicine

Docent Bengt Bergman  
University of Gothenburg  
The Institute of Medicine



## ABSTRACT

**Background:** PET/CT, positron emission tomography combined with computed tomography, with  $^{18}\text{F}$ -FDG (2-deoxy-2- $^{18}\text{F}$ fluoro-D-glucose) is well established in oncological imaging. Pulmonary carcinoid tumours may have metabolic activity, making them available for PET/CT imaging with  $^{18}\text{F}$ -FDG.

Positron-emitting isotope-labelled somatostatin analogues, such as DOTATOC (DOTA = 1,4,7,10-tetraazacyclo-dodecane-1,4,7,10-tetraacetic acid, TOC = D-Phe<sup>1</sup>-Tyr<sup>3</sup>-Octreotide), have during the last years become more widely available for imaging of abdominal neuroendocrine neoplasms by PET.

$^{68}\text{Ga}$  -DOTATOC PET is recommended by the latest version of the National Care Program for neuroendocrine abdominal tumours (2018) in Sweden, for the imaging work-up of patients with suspected or verified abdominal neuroendocrine tumour,

<https://www.cancercentrum.se/samverkan/cancerdiagnoser/neuroendokrina-buktumorer/vardprogram/gallande-vardprogram/>, [cited 2019 aug 15].

Pulmonary carcinoid tumours exhibit somatostatin receptors (SSTRs). PET/CT with  $^{68}\text{Ga}$ -DOTATOC presents the possibility of a more accurate evaluation of respiratory tract neoplasms such as pulmonary carcinoids.

**Purpose:** To differentiate pulmonary carcinoids from pulmonary hamartomas and typical from atypical pulmonary carcinoids by means of  $^{18}\text{F}$ -FDG PET and/or  $^{18}\text{F}$ -FDG PET and  $^{68}\text{Ga}$  -DOTATOC PET.

**Study I** showed that  $^{18}\text{F}$ -FDG PET/CT can distinguish pulmonary carcinoids from pulmonary hamartomas with a negative predictive value (NPV) of 92% by applying a partial volume effect corrected for the maximum standardised uptake value ( $\text{SUV}_{\text{max}}$ ) of 1.5 as a cutoff. However, these  $^{18}\text{F}$ -FDG PET measurements do not allow for the distinction between atypical and typical pulmonary carcinoids.

**Study II** evaluated  $^{18}\text{F}$ -FDG PET/CT and  $^{68}\text{Ga}$ -DOTATOC PET/CT scans in pulmonary carcinoids in correlation with SSTR expression profiles, tumour proliferation and pulmonary carcinoid subtype (typical / atypical). No correlation was found between  $^{18}\text{F}$ -FDG or  $^{68}\text{Ga}$ -DOTATOC tracer uptake in PET/CT and tumour subtype (typical pulmonary carcinoid / atypical pulmonary carcinoid). Correlation between  $^{68}\text{Ga}$ -DOTATOC and  $^{18}\text{F}$ -FDG uptake, using the tumour-to-normal-liver ratio, and immunohistochemistry in tumours, regarded as somatostatin receptor subtype 2 (or 2 and 5), was investigated. Between  $^{68}\text{Ga}$ -DOTATOC and  $^{18}\text{F}$ -FDG uptake, an inverse imaging phenotype was shown in relation to the SSTR expression

profile with high  $^{68}\text{Ga}$ -DOTATOC accumulation and low  $^{18}\text{F}$ -FDG uptake in carcinoids positive for SSTR subtypes 2 (or 2 and 5) and conversely, low  $^{68}\text{Ga}$ -DOTATOC accumulation and high  $^{18}\text{F}$ -FDG uptake in carcinoids negative for SSTR subtypes 2 (or 2 and 5).  $^{68}\text{Ga}$ -DOTATOC uptake was significantly higher for tumours expressing SSTR subtypes 2 (or 2 and 5) as compared to the tumours not expressing SSTR subtypes 2 (or 2 and 5).  $^{18}\text{F}$ -FDG uptake and Ki-67 (a marker for cell proliferation) labelling index were significantly higher for tumours not expressing SSTR subtypes 2 (or 2 and 5) as compared to the other subgroups.  $^{68}\text{Ga}$ -DOTATOC and  $^{18}\text{F}$ -FDG uptake were found to reflect tumour grading (as formulated in the study), based on Ki-67 labelling index.

**Conclusions:** It was possible to differentiate pulmonary carcinoids from hamartomas using PET measurements of the  $^{18}\text{F}$ -FDG-uptake in the tumours, corrected for partial volume effect. Clinically more aggressive, atypical pulmonary carcinoids could not be differentiated from typical pulmonary carcinoids by neither  $^{18}\text{F}$ -FDG PET/CT nor by  $^{68}\text{Ga}$ -DOTATOC PET/CT. In pulmonary carcinoid tumours, an increased  $^{68}\text{Ga}$ -DOTATOC uptake reflected somatostatin receptor subtype 2 and 5 expression. The genotypes in pulmonary carcinoids were reflected in the imaging phenotypes with inverse  $^{68}\text{Ga}$ -DOTATOC and  $^{18}\text{F}$ -FDG accumulation patterns related to the tumour somatostatin receptor profile and proliferative activity.

## SAMMANFATTNING

**Bakgrund:** PET/CT, positronemissionstomografi i kombination med datortomografi, med  $^{18}\text{F}$ -FDG (2-deoxy-2- [ $^{18}\text{F}$ ] fluoro-D-glukos) är väl etablerat vid onkologisk avbildning. Pulmonella karcinoida tumörer kan uppvisa metabolisk aktivitet, vilket gör dem tillgängliga för PET/CT-avbildning med  $^{18}\text{F}$ -FDG.

Positronemitterande isotopmärkta somatostatinanaloger, såsom DOTATOC (DOTA = 1,4,7,10-tetraazacyklo-dodekan-1,4,7,10-tetraättiksyra, TOC = D-Phe<sup>1</sup>-Tyr<sup>3</sup>-Octreotide), har under de senaste åren blivit mer allmänt tillgängliga för avbildning med PET av abdominella neuroendokrina neoplasmer.

$^{68}\text{Ga}$ -DOTATOC PET rekommenderas i den senaste versionen av Nationellt vårdprogram för neuroendokrina buktumörer (2018) i Sverige för utredningen av patienter med misstänkt eller verifierad neuroendokrin tumör i buken,

<https://www.cancercentrum.se/samverkan/cancerdiagnoser/neuroendokrina-buktumorer/vardprogram/gallande-varldprogram/>, [läst 2019-08-15].

Pulmonella karcinoida tumörer (lungkarcinoider) uppvisar somatostatinreceptorer (SSTR).  $^{68}\text{Ga}$ -DOTATOC (somatostatinanalog) PET/CT ger möjligheten till en mer exakt utvärdering av neoplasmer i luftvägarna, såsom lungkarcinoider.

**Syfte:** Att differentiera lungkarcinoider från hamartomer och typiska från atypiska lungkarcinoider med hjälp av  $^{18}\text{F}$ -FDG PET och/eller  $^{18}\text{F}$ -FDG PET och  $^{68}\text{Ga}$ -DOTATOC PET.

**Studie I** visade att  $^{18}\text{F}$ -FDG PET/CT kan skilja pulmonella karcinoider från lunghamartomer med ett negativt prediktivt värde (NPV) på 92% genom att tillämpa en partiell volymeffekt-korrigerad maximalt standardiserat värde ( $\text{SUV}_{\text{max}}$ ) på 1,5 som ett gränsvärde. Dessa  $^{18}\text{F}$ -FDG PET-mätningar medger emellertid inte separering av atypiska från typiska lungkarcinoider.

**Studie II** utvärderade  $^{18}\text{F}$ -FDG PET/CT och  $^{68}\text{Ga}$ -DOTATOC PET/CT i lungkarcinoider i korrelation med SSTR-uttrycksprofiler, tumörproliferation och lungkarcinoid-subtyp (typisk / atypisk). Ingen korrelation hittades mellan  $^{18}\text{F}$ -FDG- eller  $^{68}\text{Ga}$ -DOTATOC- upptag med PET/CT och tumörsubtyp (typisk lungkarcinoid / atypisk lungkarcinoid). Korrelation mellan  $^{68}\text{Ga}$ -DOTATOC- och  $^{18}\text{F}$ -FDG- upptag, med användning av tumör- till normalt-lever- ratio, och immunohistokemi i tumörer för somatostatinreceptorsubtyp 2 (eller 2 och 5) blev undersökt.  $^{68}\text{Ga}$ -DOTATOC- och  $^{18}\text{F}$ -FDG- upptag visade gentemot varandra en omvänd avbildningsfenotyp i förhållande till SSTR-uttrycksprofilen, med hög  $^{68}\text{Ga}$ -DOTATOC-ackumulering och lågt  $^{18}\text{F}$ -FDG-upptag i karcinoider positiva för SSTR-subtyperna 2 (eller 2 och 5) och omvänt lågt  $^{68}\text{Ga}$ -DOTATOC-ackumulering och högt  $^{18}\text{F}$ -FDG-upptag i karcinoider negativa för SSTR-subtyper 2 (eller 2 och 5).  $^{68}\text{Ga}$ -DOTATOC-upptaget var signifikant högre

för tumörer som uttryckte SSTR-subtyp 2 (eller 2 och 5) jämfört med tumörer som inte uttryckte SSTR-subtyp 2 (eller 2 och 5).  $^{18}\text{F}$ -FDG-upptaget och Ki-67 (en markör för cellproliferation) index var signifikant högre för tumörer som inte uttryckte SSTR-subtyp 2 (eller 2 och 5) jämfört med de andra subgrupperna.  $^{68}\text{Ga}$ -DOTATOC- och  $^{18}\text{F}$ -FDG- upptag visade sig återspegla tumörgradering (såsom formulerats i studien), baserat på Ki-67 index.

**Slutsats:** Det var möjligt att differentiera lungkarcinoiderna från hamartomer med användning av PET-mätningar av  $^{18}\text{F}$ -FDG-upptag i tumörerna, korrigerade för partiell volymeffekt. Kliniskt mer aggressiva atypiska lungkarcinoider kunde inte differentieras från typiska lungkarcinoider med  $^{18}\text{F}$ -FDG PET/CT eller med  $^{68}\text{Ga}$ -DOTATOC PET/CT. I lungkarcinoidtumörer reflekterade ett ökat  $^{68}\text{Ga}$ -DOTATOC-upptag uttrycket av somatostatinreceptorsubtyp 2 (eller 2 och 5). Genotyperna i lungkarcinoider återspeglades i avbildande fenotyper med invers  $^{68}\text{Ga}$ -DOTATOC- och  $^{18}\text{F}$ -FDG- ackumuleringsmönster relaterade till tumörsomatostatinreceptorprofil och proliferativ aktivitet.

## LIST OF SCIENTIFIC PAPERS

- I.  **$^{18}\text{F}$ -FDG PET/CT diagnosis of bronchopulmonary carcinoids versus pulmonary hamartomas.**  
Uhlén N, Grundberg O, Jacobsson H, Sundin A, Dobra K, Sánchez-Crespo A, Axelsson R, Kölbeck K-G.  
*Clin Nucl Med.* 2016;41:263-267.
  
- II. **Hallmarks in pulmonary endocrine tumor imaging utilizing dual tracer PET/CT with  $^{18}\text{F}$ -FDG and  $^{68}\text{Ga}$ -DOTATOC with reference to immunohistochemical somatostatin receptor profile and tumor proliferation.**  
Sundin A, Uhlén N, Dobra K, Grundberg O, Jacobsson H, Béndek M, Kölbeck K, Axelsson R, Sanchez-Crespo A. Submitted

# CONTENTS

1	INTRODUCTION.....	1
1.1	Background.....	1
1.2	Pulmonary carcinoids and hamartomas .....	1
1.3	<sup>18</sup> F-FDG PET/CT .....	2
1.4	Somatostatin receptors .....	2
1.5	<sup>68</sup> Ga-DOTATOC PET/CT.....	6
1.6	Immunohistochemistry and histopathology.....	6
1.7	Partial volume effect and quantification of tumour uptake.....	7
2	AIMS OF THIS THESIS .....	8
3	MATERIALS AND METHODS .....	9
3.1	Patients.....	9
3.2	PET imaging .....	9
3.3	PET image analysis .....	10
3.4	Partial volume correction for tracer uptake measurements.....	10
3.5	Immunohistochemistry and histopathology.....	10
3.6	Statistical analysis.....	13
4	Results.....	14
4.1	Study I.....	14
4.2	Study II .....	14
5	DISCUSSION .....	20
6	CONCLUSIONS.....	23
7	REFERENCES.....	24

## LIST OF ABBREVIATIONS

AC	Atypical pulmonary carcinoid tumour
CT	Computed tomography
DOTATOC	DOTA = 1,4,7,10-tetraazacyclo-dodecane-1,4,7,10-tetraacetic acid, TOC = D-Phe <sup>1</sup> -Tyr <sup>3</sup> -Octreotide
DOTATATE	DOTA = 1,4,7,10-tetraazacyclo-dodecane-1,4,7,10-tetraacetic acid, TATE= D-Phe <sup>1</sup> -Tyr <sup>3</sup> -Octreotate
<sup>18</sup> F	Radioactive nuclide of Fluor
<sup>18</sup> F-FDG	2-deoxy-2-[ <sup>18</sup> F]fluoro-D-glucose
<sup>18</sup> F-FDG PET/CT	Positron emission tomography with <sup>18</sup> F-FDG combined with computed tomography
<sup>68</sup> Ga	Radioactive nuclide of Gallium
<sup>68</sup> Ga -DOTATOC	<sup>68</sup> Ga-labelled DOTATOC
<sup>68</sup> Ga-DOTATATE	<sup>68</sup> Ga-labelled DOTATATE
<sup>68</sup> Ga -DOTATOC PET/CT	Positron emission tomography with <sup>68</sup> Ga -DOTATOC combined with computed tomography
<sup>68</sup> Ga-DOTA-SSA	<sup>68</sup> Ga-labelled somatostatin analogue
<sup>111</sup> In	Radioactive nuclide of Indium
IHC	Immunohistochemistry
IRS	Immunoreactive score
Ki-67	An antigen and a marker for cell proliferation.
Ki-67 labelling index	The percentage of Ki-67 positively stained cells out of the total number of cells
LCNEC	Large cell neuroendocrine carcinoma
NPV	Negative predictive value
NSCLC	Non-small cell lung carcinoma
PET	Positron emission tomography
PET/CT	Positron emission tomography combined computed tomography
PC	Pulmonary carcinoid tumour
PPV	Positive predictive value

PVE	Partial volume effect
SCLC	Small cell lung carcinoma
SSA	Somatostatin analogue
SSTR1, SSTR2, SSTR3, SSTR4, SSTR5	Somatostatin receptor subtypes
SUV	Standardised uptake value
SUV <sub>max</sub>	Maximum standardised uptake value
SUR	Standardised uptake value ratio, the ratio of activity concentration in tumour and normal tissue
TC	Typical pulmonary carcinoid tumour
VOI	Volume of interest
WHO	World Health Organisation

# 1 INTRODUCTION

## 1.1 BACKGROUND

<sup>18</sup>F-FDG PET/CT, positron emission tomography (PET) with 2-deoxy-2-[<sup>18</sup>F]fluoro-D-glucose (<sup>18</sup>F-FDG) combined with computed tomography (CT) is well established in oncological imaging and integrated into the imaging work-up of patients with suspected pulmonary carcinoid tumours (PCs). It is important to identify PCs preoperatively for treatment planning. The low incidence of PCs (they comprise 2-5% of all primary lung malignancies and 20-30% of all neuroendocrine neoplasms) makes it difficult to perform prospective studies on this type of tumour in a large patient group<sup>1-6</sup>. Neuroendocrine neoplasms exhibit somatostatin receptors (SSTRs) with heterogeneous SSTRs distribution in pulmonary neuroendocrine neoplasms<sup>7</sup>. Radiologic imaging, using radiopharmaceuticals for PET other than <sup>18</sup>F-FDG, such as <sup>68</sup>Ga-labelled somatostatin analogues (<sup>68</sup>Ga-DOTA-SSAs), reflecting the density of SSTRs in clinically suspected PC tumours, may be a helpful approach in an initial evaluation of the type of malignancy for effective clinical management of PC patient.

## 1.2 PULMONARY CARCINOIDS AND HAMARTOMAS

The current World Health Organisation (WHO) classification of tumours of the lung, pleura, thymus and heart requires grouping together PCs (typical carcinoid and atypical carcinoid tumours), the small cell lung carcinoma (SCLC) and the large cell neuroendocrine carcinoma (LCNEC) in one category of neuroendocrine tumours<sup>8</sup>. Clinically characterised by aggressiveness, typical carcinoids (TCs) are low-grade malignant, atypical carcinoids (ACs) - intermediate-grade malignant, LCNECs and SCLCs are high-grade malignant<sup>9</sup>. In separating TC from atypical AC, histopathological features, mitotic count and presence or absence of necrosis are recommended. PCs are defined as TC when the number of mitoses per 2 mm<sup>2</sup> < 2 with no sign of necrosis, and as AC when the mitotic rate is 2-10 mitoses per 2 mm<sup>2</sup> and/or with evidence of necrosis<sup>8</sup>. TCs are much more common while ACs are clinically more aggressive with a higher rate of vascular invasion, metastases and recurrences. Because of their distinctly different clinical behavior, patient management varies accordingly. While CT allows for tumour localisation and morphological characterisation of the lesion with regard to edge definition, contrast enhancement and nodal involvement, none of these radiological features is pathognomonic for any PC subtype. PCs are sometimes misdiagnosed. The majority of these tumours are centrally located (i.e. in a main, lobar or segmental bronchus), and easy to diagnose by bronchoscopy. PCs arising in distal to segmental bronchi are radiologically considered as peripheral. Peripheral PCs provide a diagnostic challenge since they cannot be assessed by bronchoscopy. If a hamartoma (the most frequent benign lung tumour) or peripheral PC presents as a small lesion, both bronchoscopic biopsy and CT-guided biopsy may be difficult. Needle biopsy may produce false negative results. It is not always easy to distinguish PCs from other tumour types by radiological imaging. Nevertheless, on a CT scan, high attenuation and high contrast-enhancement are indicative of a carcinoid tumour, whereas a hamartoma is characterised by smooth nodule edge, fat content

and popcorn like calcifications<sup>10</sup>. On chest X-ray and CT, differentiation between a malignant tumour and a hamartoma can prove difficult when the latter lacks characteristic tissue components. Also, the presence of fat in a lung nodule does not always exclude malignancy. According to the data reported in literature and experience from our Institution, in a great part of the clinically assessed cases there is a lack of characteristic radiological criteria for a hamartoma. As a result of this - a need to employ additional diagnostic methods is required. For a differential diagnosis, a further diagnostic workup is therefore often needed, usually comprising <sup>18</sup>F-FDG PET with CT (<sup>18</sup>F-FDG PET/CT)<sup>10-12</sup>.

### **1.3 <sup>18</sup>F-FDG PET/CT**

PET/CT with <sup>18</sup>F-FDG is well established in oncological imaging. Despite many publications about <sup>18</sup>F-FDG PET/CT imaging of lung malignancies, the studies include a limited number of PC patients<sup>3,13-19</sup>. There are several reports demonstrating <sup>18</sup>F-FDG avid TCs<sup>3,17,19</sup> and ACs<sup>13</sup>. ACs have a tendency to show sufficiently high <sup>18</sup>F-FDG uptake because of their higher mitotic count, while pulmonary hamartomas show no or low uptake. This can be helpful to differentiate PCs from hamartomas<sup>12</sup>. A TC with an extensive oncocytic component showing an intense <sup>18</sup>F-FDG uptake was demonstrated in individual case reports by several investigators<sup>17,19</sup>. Suemitsu et al. reported a TC with distant metastasis showing high <sup>18</sup>F-FDG uptake at the primary site and liver metastasis<sup>3</sup>. Erasmus et al. demonstrated TCs with low <sup>18</sup>F-FDG uptake as did half of the patients with TCs in a study by Krüger et al.<sup>13,15</sup>. However, the studies by Erasmus et al. and Krüger et al. were limited by their size (7 and 13 patients, respectively)<sup>13,15</sup>. <sup>18</sup>F-FDG PET/CT is considered less well suited for imaging of neuroendocrine tumours with low proliferation rate, such as PCs<sup>13,20-22</sup>. PCs are slow growing and their generally discrete <sup>18</sup>F-FDG uptake may lead to false-negative results. Further, the recent study by Panagiotidis et al. demonstrated that <sup>18</sup>F-FDG PET/CT has no clinical impact on well-differentiated neuroendocrine tumours and a moderate clinical impact on intermediate-differentiated neuroendocrine neoplasms<sup>23</sup>.

### **1.4 SOMATOSTATIN RECEPTORS**

The human SSTR subtypes are SSTR1, SSTR2, SSTR3, SSTR4 and SSTR5. For peptides like somatostatin, the binding to the receptors occurs at the extracellular loop segments and the superior parts of the transmembrane helices (Figure 1A, 1B, 1C). During evolution, receptor subtypes evolved from preceding receptors after a gene duplication. Amino acids, important for the function of the original receptor, tend to stay conserved during the divergence. The seven transmembrane helices stay highly conserved between receptor subtypes (Fig. 1A). These helices are important for the localisation of the receptor in the plasma membrane and for the transduction of the activation signal from the extracellular ligand-binding site to the intracellular side of the cell. Functionally, the ligand-binding site should be fairly well conserved in order to retain the recognition of the ligand. The presence of 2-5 subtypes, within a receptor type, is not uncommon. The different subtypes may execute various physiological effects in the body, depending on their respective tissue localisation, expression level, binding affinity for hormones and drugs, intracellular

signalling, etc. Lung neuroendocrine neoplasms have heterogeneous distribution of SSTR with decreased expression of SSTR2 and SSTR3 from low-grade/intermediate-grade (PCs) to high-grade (SCLC and LCNEC) tumours<sup>7</sup>. Among the SSTRs, SSTR subtype 2 (SSTR2) shows high expression in human neuroendocrine neoplasms<sup>24,25</sup>. The SSTR2 receptor has been proposed for evaluation with somatostatin analogues<sup>7,26,27</sup>.

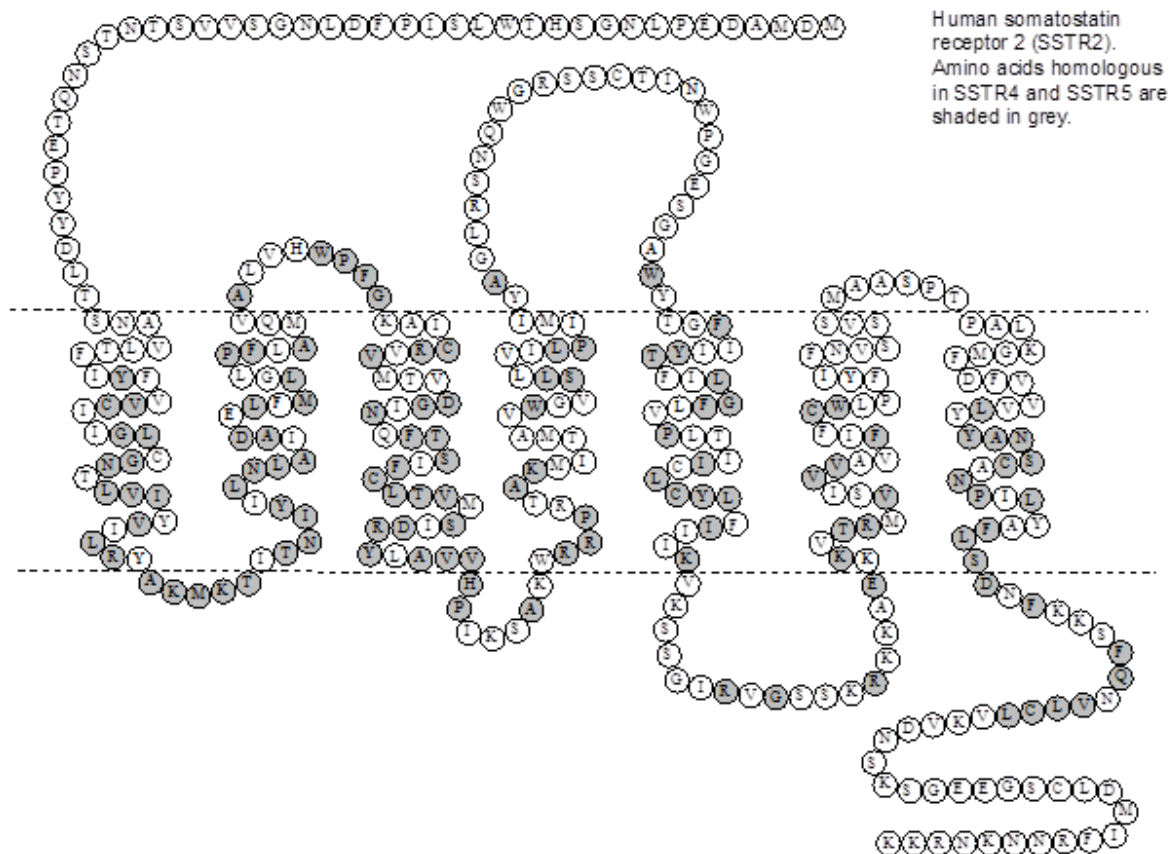


**Figure 1A.** Human somatostatin receptor subtype 2 (SSTR2). Each circle represents one amino acid. The horizontal lines define the inner and outer borders of the plasma membrane. There are seven transmembrane helices. The N-terminus, starting with a methionine (M), is situated extracellular, while C-terminal end is situated intracellular.

The human somatostatin receptor sequences were retrieved from the UniProt database.

[Retrieved 2018-07-27]. Available from: <https://www.uniprot.org/uniprot/P30874>

The 2D snakeplot of SSTR2 was retrieved from the database GPCR - SSFE 2.0

(a homology modeling resource for G-protein coupled receptors). [Retrieved 2018-07-27].

Available from: <http://www.ssfa->

[7tmr.de/ssfe2/snakes/refine\\_designer\\_neu.php?jobid=1510586369&%20name=ssr2\\_human](http://www.ssfa-7tmr.de/ssfe2/snakes/refine_designer_neu.php?jobid=1510586369&%20name=ssr2_human)

The final figure was constructed manually



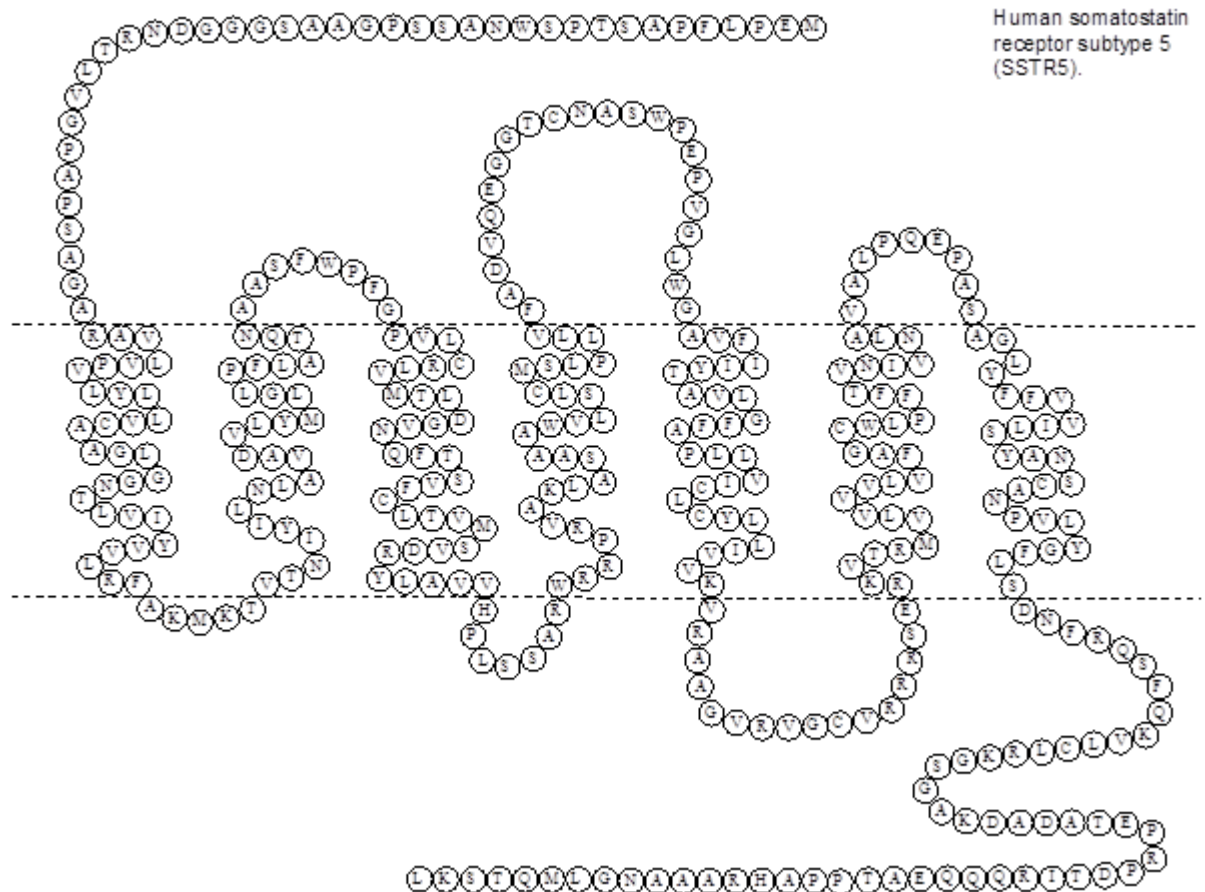


**Figure 1C.** Human somatostatin receptor subtype 5 (SSTR5). Each circle represents one amino acid.

The human somatostatin receptor sequences were retrieved from the UniProt database.

[Retrieved 2018-07-27]. Available from: <https://www.uniprot.org/uniprot/P35346>

The 2D snakeplot of SSTR5 was retrieved from the database GPCR - SSFE 2.0

(a homology modeling resource for G-protein coupled receptors). [Retrieved 2019-07-26].

Available from: <http://www.ssfa->

[7tmr.de/ssfe2/snakes/refine\\_designer\\_neu.php?jobid=1510586756&%20name=ssr5\\_human](http://www.ssfa-7tmr.de/ssfe2/snakes/refine_designer_neu.php?jobid=1510586756&%20name=ssr5_human)

The final figure was constructed manually.

## 1.5 <sup>68</sup>Ga-DOTATOC PET/CT

The somatostatin analogue (SSA), DOTATOC (DOTA = 1,4,7,10-tetraazacyclo-dodecane-1,4,7,10-tetraacetic acid, TOC = D-Phe<sup>1</sup>-Tyr<sup>3</sup>-Octreotide), shows a high affinity for SSTR2, SSTR5, and a moderate affinity for SSTR3<sup>24,28,29</sup>. Imaging with <sup>68</sup>Ga-DOTA-SSAs, reflecting SSTR expression, is well established in oncological imaging and in many centers is integrated into the imaging workup of patients with suspected or verified abdominal neuroendocrine neoplasms. <sup>68</sup>Ga-DOTA-SSAs are used extensively throughout the world in the last several years for guiding the management of many categories of neuroendocrine neoplasm patients<sup>23,30-32</sup>. Studies on PET using <sup>68</sup>Ga-DOTA-SSAs, improved the accuracy of staging of patients with neuroendocrine neoplasm and showed PET with SSAs to be equivalent or superior to SSTR scintigraphy with <sup>111</sup>In-labelled SSA in the detection of manifestations of neuroendocrine neoplasms<sup>33-36</sup>. General agreement nowadays is that PET/CT with SSAs should replace <sup>111</sup>In-labelled SSA scintigraphy in all indications in which the latter is currently being used by medical practitioners<sup>37,38</sup>. Published reports on <sup>68</sup>Ga-DOTATOC PET/CT in patients with respiratory tract neoplasms merely include a limited number of patients with PCs<sup>12,18,39,40</sup>. Menda et al. demonstrated the value of <sup>68</sup>Ga-DOTATOC PET/CT in localisation of unknown primary tumour in patients with metastatic neuroendocrine neoplasm<sup>41</sup>.

## 1.6 IMMUNOHISTOCHEMISTRY AND HISTOPATHOLOGY

The standard method to measure SSTR in vitro is through immunohistochemistry (IHC) on formalin-fixed, paraffin-embedded tissue<sup>25</sup>. IHC requires tissue samples obtained through an invasive procedure. SSTR-immunohistochemistry correlates with <sup>68</sup>Ga-DOTA-peptide PET results positively<sup>26,27,42</sup>. Similarly, it has been shown that SSTR2-immunohistochemistry also correlates well with <sup>68</sup>Ga-DOTATOC PET<sup>27</sup>.

Cancers could be characterised by their proliferative activity as measured by antibodies against the protein Ki-67, using IHC. The PCs grading based on Ki-67 labelling index is under debate. The Ki-67 index may be useful in estimating tumour progression in PCs<sup>43,44</sup>. However, even this evaluation requires tissue sampling involving biopsy or surgery. The assessment of tumour proliferation by a non-invasive PET method, by quantifying a degree of (hypothesised) correlation between the histologic grade of tumour, Ki-67 labelling index and PET/CT scan with <sup>68</sup>Ga-DOTA-SSAs, is of interest to individualise the treatment and achieve prognostic information which may have consequences for the patient's treatment<sup>23,27,45</sup>. Panagiotidis et al. stated that in line with the fact that the maximum standardised uptake value (SUV<sub>max</sub>) on <sup>68</sup>Ga-DOTATATE (DOTA, TATE= D-Phe<sup>1</sup>-Tyr<sup>3</sup>-Octreotate) PET/CT correlates with Ki-67 index, <sup>68</sup>Ga-DOTATATE can be used to assess prognosis of patients with neuroendocrine neoplasm<sup>23</sup>. On the other hand, the study by Haug et al. states a lack of significant correlation between <sup>68</sup>Ga-DOTATATE PET/CT and Ki-67 index in a neuroendocrine neoplasm patient population (only three of 27 were lung tumour patients)<sup>42</sup>. Similarly, no correlation was found between <sup>68</sup>Ga-DOTATOC uptake in neuroendocrine neoplasms and Ki-67 index in a study by Miederer et al.<sup>27</sup>. The data related to the subject is discrepant in publications.

## 1.7 PARTIAL VOLUME EFFECT AND QUANTIFICATION OF TUMOUR UPTAKE

In tumours and other tissues the standardised uptake value (SUV) is routinely used to quantify the PET tracer uptake. The SUV is achieved by dividing the radioactivity concentration (Bq/ml), for each pixel in the PET images, by the injected amount of radioactivity (Bq) per body-weight (g). As the SUV assumes a tissue density of 1g/ml, this approximation will be adequate for soft tissues but not for lung tissue.

Factors influencing the SUV are both PET camera based and patient-related<sup>46-49</sup>. An important factor influencing the SUV, the partial volume effect (PVE), has a major impact on the quantification of tumour uptake. The PVE depends on the spatial resolution of the PET system (approximately 0.5 cm) and the distribution of the tracer uptake in the tumour and surrounding tissues<sup>49</sup>. The PVE correction introduces an object size dependent quantification. The standard way to determine the impact of the PVE on PET image quantification is to use the NEMA IEC Body Phantom Set, with the same homogeneous activity concentration in all spheres<sup>50</sup>. Respiratory movements during PET acquisition also contribute to image blur. The contribution to image blur in lung tissue is up to three times larger than in soft tissues and fat<sup>47</sup>. Approaches for correcting the blurring are still under evaluation<sup>46,50</sup>.

The tracer uptake can be characterised, instead of SUV, by the standard uptake ratio (SUR), defined as the ratio of activity concentrations in tumour and, for example, aorta or normal liver. Normal liver hepatocytes are negative for all five SSTR subtypes<sup>51</sup>.

There are several problems regarding quantitative imaging using <sup>68</sup>Ga-DOTA-SSAs. The methodology for accurate in vivo quantification of <sup>68</sup>Ga-DOTA-peptide uptake is not established. It was found in a study on PET/CT with <sup>68</sup>Ga-DOTATATE and <sup>68</sup>Ga-DOTATOC that the SUV does not reflect the SSTR expression for neuroendocrine neoplasms with high tracer accumulation<sup>52,53</sup>. Moreover, measurements in tracer accumulation can be affected by the amount of administered active substance in tumours and normal tissues<sup>54</sup>. Because of the longer mean range of the <sup>68</sup>Ga positron, <sup>68</sup>Ga PET imaging has lower sensitivity and worse spatial resolution relative to <sup>18</sup>F PET imaging<sup>50</sup>. The PVE makes activity quantification more inaccurate with <sup>68</sup>Ga than <sup>18</sup>F. Unless proper corrections for the PVE are applied, quantification of <sup>68</sup>Ga-based PET imaging with SUV should be performed with caution<sup>46</sup>. In PET literature, the results of tracer uptake measurements in tumors and normal tissues are widely reported, generally without taking the PVE into consideration. Even reference value, SUV<sub>max</sub>, suggested as “cutoffs” to distinguish benign from malignant tumours, is usually presented without considering the lesion size. However, the scientifically correct way to perform a quantitative inter-patient comparative PET study, is with PVE corrected values<sup>55,56</sup>. Uncorrected SUV values merely represent the investigated cohort with the specific PET scanner and cannot be extrapolated to a general patient population. PVE corrected SUV values can be compared between patients and PET centres.

## 2 AIMS OF THIS THESIS

It is important to identify PCs preoperatively for treatment planning. So far, there are a limited number of reports evaluating the use of  $^{18}\text{F}$ -FDG-PET/CT and  $^{68}\text{Ga}$ -DOTATOC-PET/CT in patients with PCs, and within those reports the numbers of PC patients are few.

**Study I** To differentiate PCs from pulmonary hamartomas by means of  $^{18}\text{F}$ -FDG PET/CT.

To analyse whether it is possible, using PET measurements of  $^{18}\text{F}$ -FDG in the tumours, corrected for PVE, to distinguish TCs from ACs.

**Study II** To obtain, in a prospective study, PVE corrected tumour uptake measurements on PET/CT with  $^{68}\text{Ga}$ -DOTATOC and  $^{18}\text{F}$ -FDG, using the tumour-to-normal-liver SUV ratio (SUR).

To assess if  $^{18}\text{F}$ -FDG and  $^{68}\text{Ga}$ -DOTATOC accumulation in PCs correlates with tumour proliferation (Ki-67 labelling index).

To analyse whether, using PET measurements of  $^{18}\text{F}$ -FDG and  $^{68}\text{Ga}$ -DOTATOC, it is possible to distinguish TCs from ACs.

### 3 MATERIALS AND METHODS

The studies were approved by the Regional Ethical Board (2012/1921-31/1) and the Hospital's Radiation Protection Committee (K2696-2012).

#### 3.1 PATIENTS

**Study I:** A retrospective analysis of 87 out of 118 patients with a histopathologically proven diagnosis of PC or pulmonary hamartoma, surgically resected at the Karolinska University Hospital, Stockholm, Sweden between Oktober 2005 and February 2012 and who had also undergone  $^{18}\text{F}$ -FDG PET/CT preoperatively. 31 patients were excluded as they had not undergone preoperative thoracic  $^{18}\text{F}$ -FDG PET/CT. All patients were referred to  $^{18}\text{F}$ -FDG PET/CT on the suspicion of lung cancer based on chest X-ray and in some cases equivocal findings on CT. Patients with PCs rarely express elevated biochemical tumour markers and this was also the case in the present group of PC patients in whom biochemistry in this regard was normal.

The final diagnosis was based on the histopathological examination of surgical specimens. The PCs were further subclassified as TC or AC based on the World Health Organization's criteria<sup>57</sup>.

**Study II:** All patients at the Karolinska University Hospital, Stockholm, Sweden between March 2013 and September 2015 with a strong suspicion or established diagnosis of PC tumour and planned for surgical resection were asked to participate in this study. The patients were initially referred to  $^{18}\text{F}$ -FDG PET/CT on the suspicion of lung cancer based on CT. Patients with suspected PC were asked for participation in this study and were consequently referred to  $^{68}\text{Ga}$ -DOTATOC PET/CT. The time interval between the two PET examinations was 28.5 days. The final diagnosis was based on histopathological examination of surgical specimens. The PCs were subclassified as TC or AC based on the WHO's criteria<sup>8</sup>. Final patient inclusion criteria was a histopathological confirmed diagnosis of PCs from surgical specimens.

#### 3.2 PET IMAGING

All patients in study I underwent preoperative PET/CT examination with  $^{18}\text{F}$ -FDG. All patients in study II underwent two preoperative PET/CT examinations, first with  $^{18}\text{F}$ -FDG and then, within approximately 1 month, with  $^{68}\text{Ga}$ -DOTATOC. All PET/CT examinations were performed on a Biograph 64 TruePointTrueV PET/CT scanner (Siemens Medical Solutions, Erlangen, Germany).  $^{18}\text{F}$ - PET/CT was performed 1 hour after intra-venous (i.v.) injection of 4 MBq/kg body-weight of  $^{18}\text{F}$ -FDG. 3 MBq/kg body-weight of  $^{68}\text{Ga}$ -DOTATOC was injected as an intravenous bolus, the mean time of examination registration after injection was 45 min. Patients were scanned from the base of skull to proximal thighs. A low-dose CT for photon scatter correction and attenuation with a reduced reference x-ray tube electric current of 50 mA was performed before PET examination. PET examination was done directly thereafter, followed by a diagnostic quality CT. The PET acquisition conditions were

the following: 3D, 3 min per bed position, during quiet normal breathing. The PET images were reconstructed using manufacturer's 2D-OSEM algorithm (4/8 iteration/subset) using a 5 mm postreconstruction smoothing Gaussian filter; image matrix size, 168x168; slice thickness, 5 mm. The correction for scattered radiation, acquisition dead time and random coincidences was done.

### 3.3 PET IMAGE ANALYSIS

In each PET examination, volumes of interest (VOIs) were drawn to include the tumours, using the commercial software, and the SUV of the pixel with the highest radioactivity concentration ( $SUV_{max}$ ) was registered. The volume of the lesion (metabolic tumor volume for  $^{18}F$ -FDG and somatostatin receptor volume for  $^{68}Ga$ -DOTATOC) was recorded and approximated by using the ellipsoid formula and measurements of three orthogonal axes in the CT examinations. In study II, the SUR, defined as the tumor  $SUV_{max}$  divided by the mean SUV in normal liver tissue, was calculated for all patients and tracers.

### 3.4 PARTIAL VOLUME CORRECTION FOR TRACER UPTAKE MEASUREMENTS

The  $SUV_{max}$  values were corrected for PVE by applying lesion volume specific recovery coefficients, based on previous measurements, utilising a NEMA IEC body phantom filled with  $^{18}F$  and  $^{68}Ga$ , respectively<sup>50</sup>.

The six spheres of the phantom (with 1.0, 1.3, 1.7, 2.2, 2.8 and 3.7 cm inner diameter) were homogeneously filled with radiotracer ( $^{18}F$ -FDG and  $^{68}Ga$ -DOTATOC, respectively), at equal concentration, so that all PET image pixel values obtained within each sphere would have the same  $SUV = 1$ . No background activity was used. The protocol for acquisition described above was used for the phantom experiments. The PET images were reconstructed using manufacturer's 2D-OSEM algorithm (4/8 iteration/subset) using a 5 mm postreconstruction smoothing Gaussian filter; image matrix size, 168x168; slice thickness, 5 mm. VOIs corresponding with the sphere contours were automatically created for each sphere of the phantom by using the phantom CT image, and the average SUV for each VOI was recorded. PET image recovery coefficients as a function of object size were then obtained as the ratio of the expected  $SUV = 1$  for each sphere size and the measured mean SUV for each sphere size.

### 3.5 IMMUNOHISTOCHEMISTRY AND HISTOPATHOLOGY

**Study I:** The PCs were classified as TC or AC based on the World Health Organisation's criteria<sup>57</sup>. As an additional measure of proliferation, the proliferation marker Ki-67 was expressed in PCs as the percentage of positively stained cells among the total number of cells within at least 10 randomly selected high power fields.

**Study II:** Consecutive sections from formalin-fixed and paraffin-embedded tumour tissue were subjected for immunohistochemical visualisation of the SSTR subtypes, comprising SSTR 1-5, following the standard IHC protocols at the Karolinska University Hospital.

IHC reactions were independently scored by two pathologists (KD and MB), both blinded for the results of PET analysis. IHC reactions were independently analysed by counting multiple regions of highest labelling density. SSTR subtypes 1 and 3 were not significantly expressed in any individual of this cohort.

The scoring parameters included the percentage of positive cells where 0 corresponds to no positive cells; 1≤10% positive cells; 2=11-50% positive cells; 3=51-80% positive cells; 4>80% positive cells. The intensity of staining was graded 0= no staining; 1= mild staining intensity; 2= moderate staining intensity; 3= intense staining reaction. Immunoreactive score (IRS) was calculated by multiplying the percentage of positive cells with the staining intensity. The resulting IRS ranged 0 to 12, and was stratified as [0-1]= negative immunoreactivity, [2-3]= mild immunoreactivity, [4-8]= moderate immunoreactivity and [9-12]= strong immunoreactivity. As the final step of the evaluation, the specific SSTR subtype immunohistopathological expression was then considered positive if  $IRS \geq 4$  or negative if  $IRS < 4$ .

Tumour classification in TC or AC was performed from the individual pathological-anatomical diagnosis (based on the World Health Organisation's criteria<sup>8</sup>). The Ki-67 labelling index was determined and expressed as the percentage of positively stained cells out of the total number of cells within at least 10 high power fields.

The PC were then subclassified into three groups according to their Ki-67 labelling index ; the Low grade group (corresponding to tumour cells with Ki-67 <2%); the Intermediate grade (corresponding to tumour cells with Ki-67 [2-20%]) and the High grade (Ki-67 >20%) (Table 1). To note as a terminology issue – the terms Low grade, Intermediate grade, High grade, devised and used in the text (Table 1), are not the same as tumour characteristics by aggressiveness, where TCs are considered to be low-grade, ACs - intermediate-grade, and LCNECs/SCLCs high-grade malignant<sup>9</sup>.

**Table 1.** Patient characteristics, histopathology and devised tumour grading

Patient (age, years; sex)	Histopatho- logical examination	Ki-67 (%)	Tumour group based on KI-67 labelling index
1. (77; F)	TC	1	Low grade
2. (18; M)	TC	3	Intermediate grade
3. (39; F)	TC*	<5	Intermediate grade
4. (55; M)	TC	3	Intermediate grade
5. (55;M)	TC	3	Intermediate grade
6. (73; F)	AC*	10	Intermediate grade
7. (52; M)	AC	1	Low grade
8. (71; M)	TC*	<2	Low grade
9. (33; F)	TC	3	Intermediate grade
10. (74; M)	TC	1	Low grade
11. (81; F)	TC	<2	Low grade
12. (71; F)	TC	8	Intermediate grade
13. (62; M)	TC	1	Low grade
14. (43; M)	TC	<1	Low grade
15. (44; M)	TC	2	Intermediate grade
16. (40; F)	TC	10	Intermediate grade
17. (48; M)	TC	4	Intermediate grade
18. (73; M)	TC	5	Intermediate grade
19. (76; M)	TC	1	Low grade
20. (69; M)	AC	7	Intermediate grade
21. (68; M)	TC	<1	Low grade
22. (71; F)	AC*	45	High grade
23. (72; F)	TC	1	Low grade
24. (63; F)	TC	<1	Low grade
25. (44; M)	AC	<2	Low grade
26. (19; M)	TC	4	Intermediate grade

\*, with metastasis; AC, atypical carcinoid; TC, typical carcinoid; Low grade, Ki-67 labelling index <2%; Intermediate grade, Ki-67 labelling index [2-20%]; High grade, Ki-67 labelling index >20%

### 3.6 STATISTICAL ANALYSIS

**Study I:** The PVE corrected PET results were grouped, as PCs and hamartomas, and the  $SUV_{max}$ . Statistical differences between groups were tested with  $p < 0.05$  as significant level for all tests. The statistical differences in  $SUV_{max}$  between hamartomas and PCs and between hamartomas and periferal PCs were investigated using a t-test. To evaluate statistical differences in  $SUV_{max}$  between central and peripheral PCs as well as between TCs and ACs a non-parametric Wilcoxon rank sum test was used. For pooled PCs the linear correlation between the  $SUV_{max}$  and Ki-67 labelling index was tested.

**Study II:** The tracer uptake was characterised by the standard uptake ratio (SUR), defined in the study as the ratio of activity concentrations in tumour and normal liver tissue (the tumor  $SUV_{max}$  divided by the mean SUV in normal liver tissue). The relationships between PET measurements and PC SSTR profile, grading (based on KI-67 labelling index) and type were analysed using one-way analysis of variance (ANOVA) with  $p < 0.05$  as significant level.

## 4 RESULTS

### 4.1 STUDY I

51 patients with pulmonary hamartomas and 36 patients with PCs were evaluated in this study. The tumour sizes varied between 7 and 53 mm. The mean (range) size for hamartomas was 16 (7-34) mm, for PCs 25 (8-53) mm.

Among the PCs (mean  $SUV_{max}$  3.9), 25 were classified as TC (mean  $SUV_{max}$  3.9), six as TC with lymph node metastasis (mean  $SUV_{max}$  3.9), two as AC and three as AC with lymph node metastasis. In total, 31 patient in category pooled TCs (mean  $SUV_{max}$  3.8), and five patients in pooled ACs (mean  $SUV_{max}$  5.0). Of 36 pooled (periferal and central) PCs, 23 were centrally located (mean  $SUV_{max}$  4.0) and 13 (eleven TCs, one AC and one AC with metastasis) peripherally located (mean  $SUV_{max}$  3.9). Compared to the pulmonary hamartomas (mean  $SUV_{max}$  1.4), the PVE corrected  $SUV_{max}$  was significantly higher in the pooled PCs ( $p \leq 0.00001$ ), and in the peripheral PCs ( $p \leq 0.00001$ ). No statistically significant difference was found in  $SUV_{max}$  at group level between centrally and peripherally located PCs (a non parametric Wilcoxon rank sum test,  $p = 0.8$ ).

The  $SUV_{max}$  in the ACs and TCs was similar because of the large variation in the data (mean  $\pm$  standard deviation,  $5.0 \pm 2.6$  and  $3.8 \pm 1.9$ , respectively) ( $p = 0.11$ ), with similar results when testing for differences between ACs and TCs with metastasis.

The Ki-67 was lower in TCs (with and without metastasis) (mean 2%, range 0 -12%), than for the ACs (with and without metastasis) (mean 10%, range 3-20%), ( $p = 0.0054$ ). No correlation was found between  $SUV_{max}$  for pooled PCs and Ki-67 labelling index (linear coefficient of determination  $R^2 = 0.003$ ).

A  $SUV_{max}$  of 1.5, similar to the average  $SUV_{max}$  for the hamartomas, was applied as a cutoff for malignancy.

The resulting sensitivity, specificity, positive predictive value (PPV) and negative predictive value (NPV) for  $^{18}F$ -FDG PET/CT to differ PCs from hamartomas were 92%, 69%, 67% and 92%, respectively.

### 4.2 STUDY II

Histopathological examination resulted in 21 patients with TC and five patients with AC (Table 1). Four patients had metastases. Two patients showed spread disease with distant metastases: one with liver metastases and the other with brain metastases; whereas two patients had regional lymph node metastases.

Assessment of lung lesions in our study comprised an evaluation of Ki-67 labelling index and immunohistopathological expression of SSTRs in PCs and PET/CT for findings of focally increased radiotracer ( $^{68}Ga$ -DOTATOC and  $^{18}F$ -FDG) uptake those are correlated to the IHC and histopathological examination.

Figure 2 shows the distribution of PET derived SUR for  $^{68}\text{Ga}$ -DOTATOC and  $^{18}\text{F}$ -FDG as a function of histopathological tumour classification (TC/AC). PET/CT could not distinguish ACs from TCs. The tracer accumulation in TCs and ACs were similar for  $^{68}\text{Ga}$ -DOTATOC, median SUR 4.6 and 4.8, respectively ( $p>0.05$ ). Likewise, the tracer accumulation in TCs and ACs were similar for  $^{18}\text{F}$ -FDG, median SUR 1.4 and 2.4, respectively ( $p>0.05$ ). However, in the TCs the  $^{68}\text{Ga}$ -DOTATOC SUR was significantly higher than the  $^{18}\text{F}$ -FDG SUR ( $p=0.0006$ ), but not in AC ( $p>0.05$ ).

The outcome for the IHC results and the three respective receptor subtypes, SSTR2, SSTR4 and SSTR5 were grouped in combinations positive (+) or negative (-) for subtypes [SSTR2, SSTR4, SSTR5] with the following results: [---],  $n=3$ ; [+--],  $n=14$ ; [++-],  $n=2$ ; [+++],  $n=6$  and [-+-],  $n=1$ .

SSRT subtypes 1 and 3 were not significantly expressed in any of the patients of this cohort.

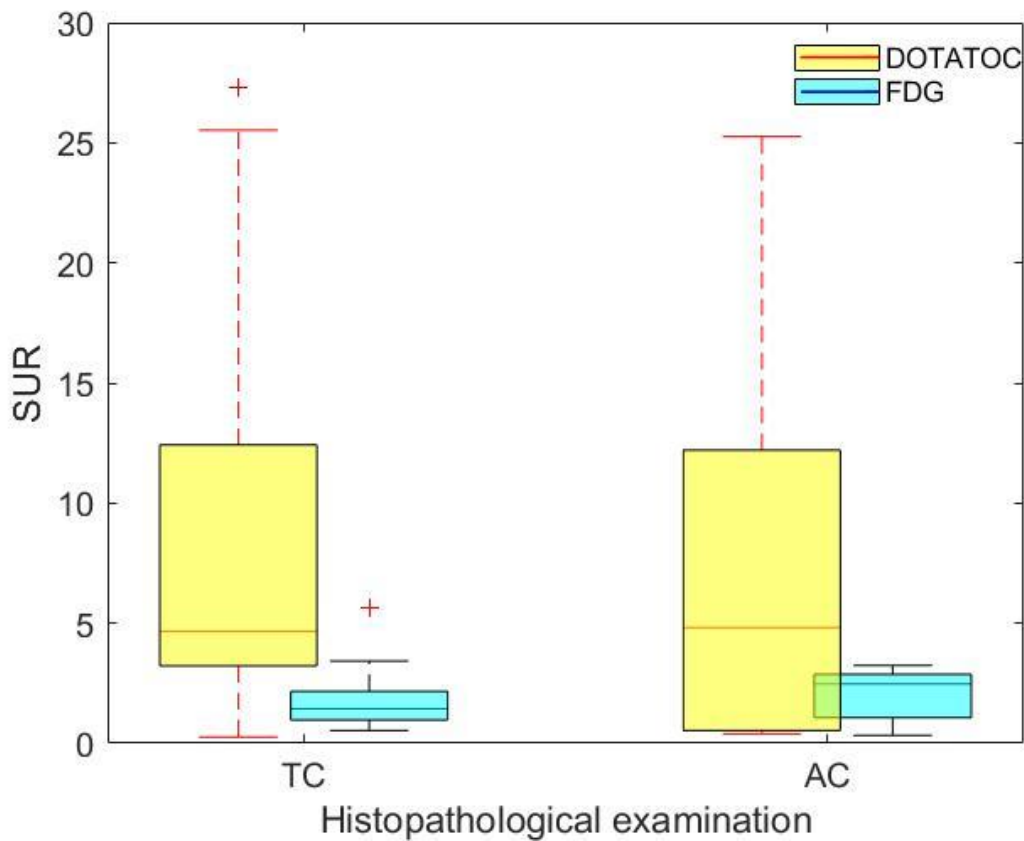


**Figure 2.** Distribution of PET image derived standard uptake ratios (SUR) of  $^{68}\text{Ga}$ -DOTATOC and  $^{18}\text{F}$ -FDG in PCs, grouped according to histopathological examination as typical (TC) and atypical (AC) carcinoids. The median of the distribution is represented by the line inside the box. An outlier is indicated with a cross. The error bars represent standard deviation of the group.

Table 2 shows the PET image derived mean SUR values for  $^{68}\text{Ga}$ -DOTATOC and  $^{18}\text{F}$ -FDG for the different combinations of SSTR subtype expression.

**Table 2.** The distribution of the mean SUR in tumours across different combinations of SSTR expression and tumour grading (Low grade, Ki-67 <2%; Intermediate grade, Ki-67 [2-20%]; High grade, Ki-67 >20% ) in tumours for  $^{68}\text{Ga}$ -DOTATOC and  $^{18}\text{F}$ -FDG.

SSTR [SSTR2,SSTR4,SSTR5]	SUR for $^{68}\text{Ga}$ -DOTATOC	SUR for $^{18}\text{F}$ -FDG
[+++] Low+Intermediate+High grade	11.5	1.4
[+++] Low grade	15.8	1.4
[+++] Intermediate grade	3.1	1.5
[+++] High grade	NA	NA
[+--] Low+Intermediate+High grade	9.9	1.6
[+--] Low grade	8.6	1.3
[+--] Intermediate grade	10.6	1.7
[+--] High grade	NA	NA
[+-+] Low+Intermediate+High grade	5.9	2.0
[+-+] Low grade	5.9	2.0
[+-+] Intermediate grade	NA	NA
[+-+] High grade	NA	NA
[---] Low+Intermediate+High grade	0.5	2.5
[---] Low grade	0.6	1.3
[---] Intermediate grade	0.4	2.8
[---] High grade	0.5	3.4
[-+-] Low+Intermediate+High grade	0.3	5.7
[-+-] Low grade	NA	NA
[-+-] Intermediate grade	0.3	5.7
[-+-] High grade	NA	NA

NA, not applicable

The  $^{68}\text{Ga}$ -DOTATOC SUR was significantly higher for tumours positive for SSTR subtypes 2 and SSTR subtypes (2 and 5) as compared to tumours not expressing these SSTR subtypes ( $p=0.037$ ). An inverse correlation was found for  $^{18}\text{F}$ -FDG, where the mean SUR value in tumours with positive expression of the SSTR subtypes 2 and SSTR subtypes (2 and 5) was significantly lower than in those with negative expression ( $p=0.005$ ). This relation between  $^{68}\text{Ga}$ -DOTATOC and  $^{18}\text{F}$ -FDG SUR and SSTR profile is also demonstrated in Figure 3. This figure shows a heatmap of the mean tumour SUR for  $^{68}\text{Ga}$ -DOTATOC and  $^{18}\text{F}$ -FDG for the different SSTR subtypes. Figure 3 clearly reveals that the tumour uptake patterns of  $^{68}\text{Ga}$ -

DOTATOC and  $^{18}\text{F}$ -FDG show an inverse imaging phenotype in relation to the SSTR subtype expression. Positive SSTR subtype 2 (or 2 and 5) expression profile is related to high  $^{68}\text{Ga}$ -DOTATOC accumulation and low  $^{18}\text{F}$ -FDG uptake and conversely, negative SSTR 2 (or 2 and 5) expression results in low  $^{68}\text{Ga}$ -DOTATOC accumulation and high  $^{18}\text{F}$ -FDG uptake ( $p < 0.05$ ).

Ki-67 labelling index was significantly higher for tumors not expressing SSTR 2 and 5 as compared to the other subgroups, [++], [+-] and [+-] ( $p = 0.03$ ).

According to the tumour subclassification, as formulated in the study with respect to Ki-67 labelling index, 12 patients were classified as Low grade group, 13 patients as Intermediate grade group and only one patient as High grade group (Table 1). Figure 4 shows the distribution of  $^{68}\text{Ga}$ -DOTATOC SUR and  $^{18}\text{F}$ -FDG SUR as a function of the subclassification with respect to Ki-67 labelling index grading, and illustrates the inverse imaging phenotype of  $^{68}\text{Ga}$ -DOTATOC and  $^{18}\text{F}$ -FDG regarding their respective accumulation in High and Low grade tumours ( $p < 0.01$ ).

Table 2 reveals differences in the relation between the accumulation of  $^{68}\text{Ga}$ -DOTATOC and  $^{18}\text{F}$ -FDG in PCs, grouped according to their grading (subclassification) and SSTR expression profile. The groups of Low/Intermediate grade PCs with strong SSTR 2 (or 2 and 5) expression presented phenotypes characterised by a strong  $^{68}\text{Ga}$ -DOTATOC accumulation and very low  $^{18}\text{F}$ -FDG metabolic avidity ( $p = 0.006/0.002$ ). The groups of PCs subclassified as Intermediate/High grade with no SSTR 2 and 5 expression showed a strong  $^{18}\text{F}$ -FDG metabolic avidity and very low  $^{68}\text{Ga}$ -DOTATOC accumulation ( $p = 0.016$ ). The group of Low grade PCs with no SSTR 2 and 5 expression showed both low accumulation of  $^{68}\text{Ga}$ -DOTATOC and low  $^{18}\text{F}$ -FDG avidity.

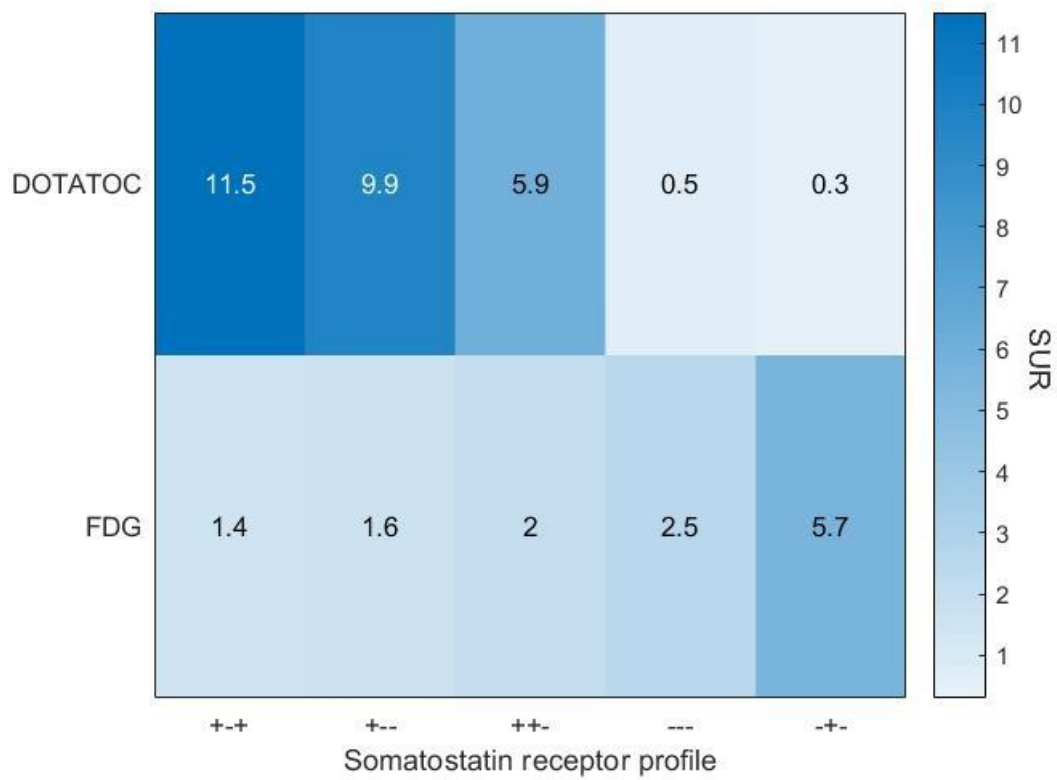


**Figure 3.** Heatmap of the mean tumour SUR for  $^{68}\text{Ga}$ -DOTATOC and  $^{18}\text{F}$ -FDG in patients with similar somatostatin receptor (SSTR) subtype expression profile, positive (+) or negative (-) for subtypes [SSTR2, SSTR4, SSTR5].

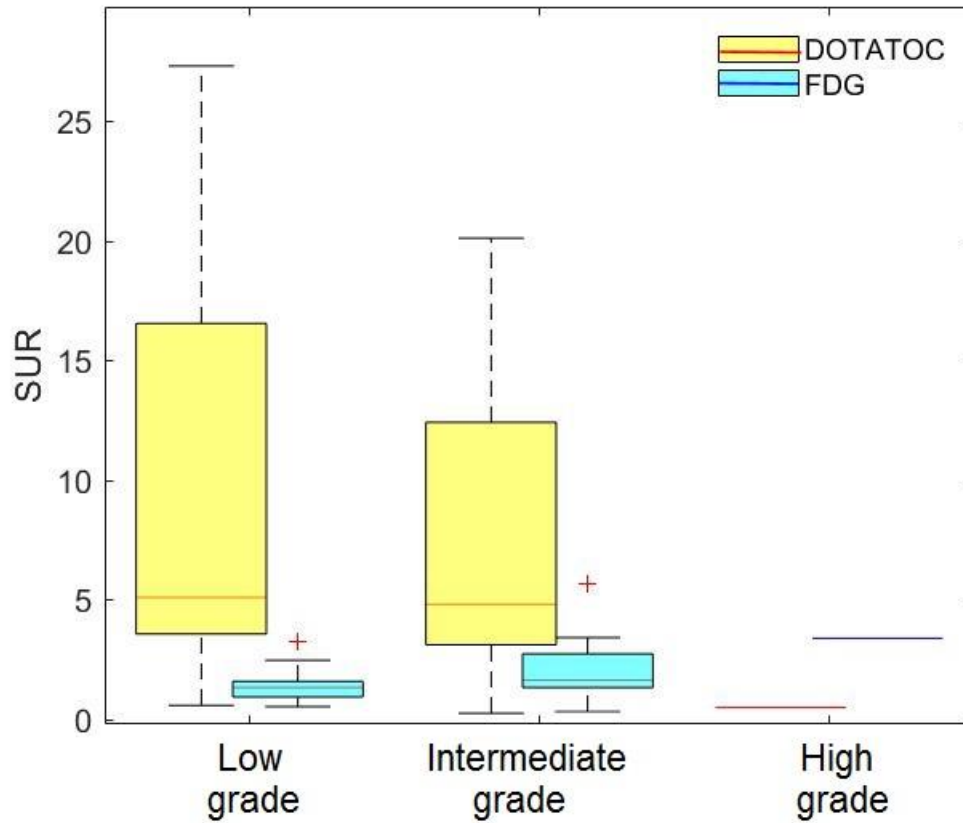


**Figure 4.** Distribution of PET image derived SUR of  $^{68}\text{Ga}$ -DOTATOC and  $^{18}\text{F}$ -FDG stratified according to the tumour classification with respect to Ki-67 labelling index. The median of the distribution is represented by the line inside the box. An outlier is indicated with a cross. The error bars represent standard deviation of the group.

## 5 DISCUSSION

**Study I:** Since the diagnosis was not achieved preoperatively, it became apparent afterwards that the surgical resection had been unnecessary in all 51 patients with benign lung pathology. Due to the increasing use of high spatial resolution multidetector CT, a substantial number of lung lesions are detected which are in need of characterisation<sup>58</sup>. For each lesion, its nature and malignancy potential must be assessed radiologically by evaluating the lesion size, tumour outline (smooth, rough, spiculated), the presence of calcifications and fat, signs of infiltration into adjacent structures, enlarged regional lymph nodes and distant metastases. Management strategies for solitary lung lesions include follow-up CT, <sup>18</sup>F-FDG PET/CT and /or biopsy.

While centrally located carcinoids are frequently symptomatic and easily assessable for diagnostic biopsy, up to 20% of carcinoids show peripheral location and appear radiologically as a solitary pulmonary nodule. These lesions are a diagnostic challenge, presenting difficulties for cytological and histopathological verification by CT-guided percutaneous needle biopsy<sup>59</sup>. Peripherally located carcinoids (13 patients) in our study were distinguished from lesions of benign origin as based on their mean  $SUV_{max}$  on <sup>18</sup>F-FDG PET<sup>55</sup>. PCs have traditionally been described as tumours with slow growth and low metabolic activity with low or even absent <sup>18</sup>F-FDG uptake<sup>13</sup>. Early <sup>18</sup>F-FDG PET studies showed low sensitivity for detection of PCs and the method has therefore been considered to have a limited role in the diagnostic work-up of these tumours. However, PCs can be <sup>18</sup>F-FDG avid to indicate malignancy<sup>14-18,20</sup>. The present results show that there was significantly higher <sup>18</sup>F-FDG uptake in PCs than in hamartomas and with a negative predictive value (NPV) of 92%, the risk of missing a PC is low<sup>55</sup>. A retrospective evaluation of the visual grading of the <sup>18</sup>F-FDG uptake in 16 subsequently resected PCs, found an overall 75% sensitivity of <sup>18</sup>F-FDG PET to detect PCs, with a trend towards higher sensitivity for the 5 ACs (80%) as compared to the 11 TCs (73%)<sup>16</sup>. Data from a study including 29 PCs (23 TCs and 6 ACs), showed that the mean  $SUV_{max}$  on <sup>18</sup>F-FDG PET in ACs was significantly higher than in TCs, 8.1 and 2.7 respectively<sup>60</sup>. Indeed, the  $SUV_{max}$  of <sup>18</sup>F-FDG did not differentiate the 26 TCs from the 5 ACs in our study<sup>55</sup>.

The size of the lesions in our study varied between 7 and 53 mm, where the size of the the smallest is similar to the intrinsic PET system spatial resolution used (6 mm full width at half maximum in the center of the field of view). It is known that quantitative measurement of SUV in tumours is highly dependent on lesion size<sup>61</sup>, and the PVE has a major effect on this measurement. Lesions below or close to the intrinsic spatial resolution of PET cameras might be detected, but show an apparent <sup>18</sup>F-FDG uptake much lower than the actual radioactivity concentration.

<sup>18</sup>F-FDG uptake in the tumour higher than that of the normal mediastinal blood pool is often used as an indication of pulmonary tumours<sup>61</sup>. To establish cutoff for positive <sup>18</sup>F-FDG uptake in our study, two factors were considered more relevant: the NPV of <sup>18</sup>F-FDG PET and the mean  $SUV_{max}$  for hamartomas. The cutoff of 1.5 for positive radiotracer uptake

influenced the NPV (92%) in our analysis. There are strengths with our study but there are also limitations. The advantages are that the present study allows for better statistical power as the study comprises a large number of patients. We have also corrected the SUV measurements for the PVE to enable a more precise quantification of  $^{18}\text{F}$ -FDG uptake and make the comparisons between tumour subgroups more accurate. However, ACs could not be differentiated from TCs. The limitations are the retrospective nature of our analysis and, consequently, that the acquired PET data are based on an examination protocol without breathing gating in order to make the SUV measurements even more precise. The relatively low PPV (67%) indicated a fairly high rate of false-positive results, but one can be confident that  $^{18}\text{F}$ -FDG negative PET corresponds with a cancer-free status.

**Study II:** In this prospective study, the accumulation of  $^{68}\text{Ga}$ -DOTATOC and  $^{18}\text{F}$ -FDG in PCs was compared and correlated with their immunohistochemical SSTR profile, grade according to Ki-67 and tumour type (TC/AC). This study included 26 verified PCs. The low incidence of PCs makes it difficult to perform prospective studies in large patient groups. Previously published reports on  $^{68}\text{Ga}$ -DOTATOC PET/CT of respiratory tract neoplasms included a limited number of patients with PCs<sup>12,18,39,40</sup>. The results of the present study in 26 patients should therefore be regarded in this perspective.

Consistent with previous reports<sup>62</sup>, the Ki-67 in our cohort showed large variations, ranging 1 to 45% (Table 1). Currently, Ki-67 labelling index is not clinically recommended to reliably differentiate between low-grade lung neuroendocrine tumours (TCs) and intermediate-grade lung neuroendocrine tumours (ACs). There are also several problems regarding the utility of Ki-67 labelling index due to both biological and methodological reasons. The sampling error in connection with biopsy may, because of tumour heterogeneity, lead to varying results and the Ki-67 labelling index and the tumour can also change over time. Earlier reports on the relationship between the tumour  $^{68}\text{Ga}$ -DOTA-SSAs accumulation and tumour grade have also shown large discrepancies<sup>23,27,42,45</sup>. This may be due to the use of different immunohistochemical techniques and counting methods, together with a lack of consensus regarding the Ki-67 index cutoff values and varying characterisation of lung neuroendocrine neoplasms<sup>63,64,65</sup>. The role of Ki-67 labelling index in tumour grading, as well as an independent prognostic parameter in predicting survival, is to date not well established<sup>62,66,67</sup>. Additional prospective studies are therefore warranted to generate more data on Ki-67 in lung neuroendocrine tumours for purposes of staging and prognosis<sup>68</sup>. DOTATOC, as reported in literature, shows a high affinity for SSTR2 and SSTR5<sup>24,28,29</sup>. This was confirmed in the present study. For measurements of tracer accumulation in the tumours we applied SUR, which was based on the tumour-to-normal liver ratio. The normal liver tissue was chosen as the reference because of its low tracer uptake variation between patients. In our cohort, the  $^{68}\text{Ga}$ -DOTATOC accumulation was positively correlated with the immunohistochemical expression of SSTR2 and co-expression of SSTR subtypes 2 and 5, in line with previously published results<sup>24,26-29,42</sup>. In our study, the  $^{68}\text{Ga}$ -DOTATOC accumulation was found to decrease with increasing PC grading and inversely the  $^{18}\text{F}$ -FDG avidity increased with increasing PC grading. These results are in accordance with previous

publications<sup>20,69</sup>. For neuroendocrine neoplasms in general, low-grade tumours show high <sup>68</sup>Ga-DOTA-SSA accumulation and low <sup>18</sup>F-FDG uptake, with the reverse situation in high-grade neuroendocrine neoplasms. Table 2 in our study shows an inverse uptake pattern between <sup>68</sup>Ga-DOTATOC and <sup>18</sup>F-FDG in relation to the PCs SSTR expression profile and tumour grading genotypes. Even though low-grade PCs are being considered less well suited for tumour detection by <sup>18</sup>F-FDG-PET/CT, most tumours in the present study showed some degree of <sup>18</sup>F-FDG uptake. Then PET with somatostatin analog is of limited value in patients with high-grade neuroendocrine neoplasms, <sup>18</sup>F-FDG PET may be more suitable. Thus, whole-body PET/CT combining <sup>68</sup>Ga-DOTATOC and <sup>18</sup>F-FDG opens the possibility to characterise different NET subtypes, and to identify tumour heterogeneity, by quantifying SSTR expression and tumour metabolism, to individualise the treatment and, although not applicable in the present cohort, also achieve prognostic information. Different PC accumulation could theoretically be encountered with the use of different <sup>68</sup>Ga-DOTA-SSA preparations with varying affinities for the different SSTR subtypes.

As initially discussed, this PET/CT study was performed in a small patient cohort and this limits the statistical power for some of the analyses. Also, the full spectrum of immunohistochemical SSTR profiles was not represented (SSTR subtypes 1 and 3 were not significantly expressed in any individual of this cohort) and the acquired PET data are based on an examination protocols without breathing gating.

Current WHO classification of tumours of the lung, pleura, thymus and heart requires grouping together PCs (AC and TC), SCLC and LCNEC in one neuroendocrine tumors category<sup>8</sup>. On molecular basis, however, LCNEC, SCLC and PCs are separate biological entities<sup>9</sup>. The alternative view suggests that TC and AC have a latent propensity for progression towards high-grade neuroendocrine neoplasms, by evolution of AC to SCLC and TC to LCNEC, according to the concept of secondary high-grade neuroendocrine neoplasms developing from preexisting PCs<sup>63,70</sup>. Molecular mechanisms of SSTR physiology and pathogenesis of neuroendocrine neoplasm are under investigation as a part in the development strategies in diagnosis and treatment of neuroendocrine tumours<sup>71,72</sup>. The recent recommendations by the European Neuroendocrine Tumor Society, advocate a multidisciplinary approach and long-term follow-up for TC and AC<sup>73</sup>. In this framework, dual tracer PET/CT in clinically suspected PCs, reflecting tumour SSTR density with <sup>68</sup>Ga-DOTATOC, and tumour metabolism with <sup>18</sup>F-FDG, can be helpful for imaging diagnosis and staging and to acquire prognostic information for treatment individualisation and follow up.

## 6 CONCLUSIONS

**Study I:** It was possible to discriminate PCs from pulmonary hamartomas using  $^{18}\text{F}$ -FDG PET measurements of  $^{18}\text{F}$ -FDG uptake by applying a PVE-corrected  $\text{SUV}_{\text{max}}$  of 1.5 as cutoff in the tumours.

$^{18}\text{F}$ -FDG PET/CT can not distinguish ACs from TCs.

**Study II:**  $^{18}\text{F}$ -FDG and  $^{68}\text{Ga}$ -DOTATOC PET measurements do not allow for separating ACs from TCs.  $^{18}\text{F}$ -FDG and  $^{68}\text{Ga}$ -DOTATOC accumulation (devised as standardise uptake ratio) was similar in TCs and ACs, although in TCs the  $^{68}\text{Ga}$ -DOTATOC SUR was significantly higher than the  $^{18}\text{F}$ -FDG SUR, but not in ACs.

The PC genotypes were reflected in the imaging phenotypes with inverse  $^{68}\text{Ga}$ -DOTATOC and  $^{18}\text{F}$ -FDG accumulation patterns. The degree of  $^{68}\text{Ga}$ -DOTATOC and  $^{18}\text{F}$ -FDG uptake was found to reflect the PC's individual combinations of immunohistochemical SSTR profile and tumour grading based on Ki-67 labelling index.

## 7 REFERENCES

1. Jindal T, Kumar A, Venkitaraman B, et al. Role of  $^{68}\text{Ga}$ -DOTATOC PET/CT in the evaluation of primary pulmonary carcinoids. *Korean J Intern Med* 2010;25:386-91.
2. Modlin IM, Sandor A. An analysis of 8305 cases of carcinoid tumors. *Cancer* 1997;79:813-29.
3. Suemitsu R, Maruyama R, Nishiyama K, et al. Pulmonary typical carcinoid tumor and liver metastasis with hypermetabolism on 18-fluorodeoxyglucose PET: a case report. *Ann Thorac Cardiovasc Surg* 2008;14:109-11.
4. Pusceddu S, Catena L, Valente M, et al. Long-term follow up of patients affected by pulmonary carcinoid at the Istituto Nazionale Tumori of Milan: a retrospective analysis. *J Thorac Dis* 2010;2:16-20.
5. Hauso O, Gustafsson BJ, Kidd M, et al. Neuroendocrine tumor epidemiology. Contrasting Norway and North America. *Cancer* 2008;113:2655-68.
6. Yao JC, Hassan M, Phan A, et al. One hundred years after "carcinoid": epidemiology of and prognostic factors for neuroendocrine tumors in 35,825 cases in the United States. *J Clin Oncol* 2008;26:3063-72.
7. Righi L, Volante M, Tavaglione V, et al. Somatostatin receptor tissue distribution in lung neuroendocrine tumours: a clinicopathologic and immunohistochemical study of 218 'clinically aggressive' cases. *Ann Oncol* 2010;21:548-555.
8. Travis WD, Brambilla E, Burke AP, et al. WHO classification of tumours of the lung, pleura, thymus and heart. Lyon, IARC Press; 2015.
9. Travis W D, Brambilla E, Nicholson AG, et al., Classification of Lung Tumors. Impact of Genetic, Clinical and Radiologic Advances Since the 2004 Classification. *J Thorac Oncol* 2015;10:1243-60.
10. Meisinger QC, Klein JS, Butnor KJ, et al. CT features of peripheral pulmonary carcinoid tumors. *AJR* 2011;197:1073-80.
11. Ko JM, Jung JI, Park SH, et al. Benign tumors of the tracheobronchial tree: CT-pathologic correlation. *AJR* 2006;186:1304-13.
12. Kumar A, Jindal T, Dutta R, et al. Functional imaging in differentiating bronchial masses: an initial experience with a combination of  $^{18}\text{F}$ -FDG PET-CT scan and  $^{68}\text{Ga}$  DOTA-TOC PET-CT scan. *Ann Nucl Med* 2009;23:745-51.
13. Erasmus JJ, McAdams HP, Patz EF, et al. Evaluation of primary pulmonary carcinoid tumors using FDG PET. *AJR* 1998;170:1369-73.
14. Lin J-H, Yen R-F, Hung G-U, et al. Pulmonary carcinoid tumor on fluorine-18-FDG PET imaging. *Ann Nucl Med Sci* 2000;13:67-70.
15. Krüger S, Buck AK, Blumstein NM, et al. Use of integrated FDG PET/CT imaging in pulmonary carcinoid tumours. *J Intern Med* 2006;260:545-50.
16. Daniels CE, Lowe VJ, Aubry M-C, et al. The utility of fluorodeoxyglucose positron emission tomography in the evaluation of carcinoid tumors presenting as pulmonary nodules. *Chest* 2007;131:255-60.
17. Kadowaki T, Yano S, Araki K, et al. A case of pulmonary typical carcinoid with an

extensive oncocytic component showing intense uptake of FDG. *Thorax* 2011;66:361-62.

18. Jindal T, Kumar A, Venkitaraman B, et al. Evaluation of the role of [<sup>18</sup>F]FDG-PET/CT and [<sup>68</sup>Ga]DOTATOC-PET/CT in differentiating typical and atypical pulmonary carcinoids. *Cancer Imaging* 2011;11:70-5.

19. Tanabe Y, Sugawara Y, Nishimura R, et al. Oncocytic carcinoid tumor of the lung with intense F-18 fluorodeoxyglucose (FDG) uptake in positron emission tomography-computed tomography (PET/CT). *Ann Nucl Med* 2013;27:781-85.

20. Kayani I, Bomanji JB, Groves A, et al. Functional imaging of neuroendocrine tumors with combined PET/CT using <sup>68</sup>Ga-DOTATE (DOTA-DPhe<sup>1</sup>, Tyr<sup>3</sup>-octreotate) and <sup>18</sup>F-FDG. *Cancer* 2008;112:2447-55.

21. Tatci E, Ozmen O, Gokcek A, et al. <sup>18</sup>F-FDG PET/CT rarely provides additional information other than primary tumor detection in patients with pulmonary carcinoid tumors. *Ann Thorac Med* 2014;9:227-31.

22. Binderup T, Knigge U, Loft A, et al. <sup>18</sup>F-fluorodeoxyglucose positron emission tomography predicts survival of patients with neuroendocrine tumors. *Clin Cancer Res* 2010;16:978-85.

23. Panagiotidis E, Alshammari A, Michopoulou S, et al. Comparison of the impact of <sup>68</sup>Ga-DOTATATE and <sup>18</sup>F-FDG PET/CT on clinical management in patients with neuroendocrine tumors. *J Nucl Med* 2017;58:91-6.

24. Reubi J C, Schonbrunn A. Illuminating somatostatin analog action at neuroendocrine tumor receptors. *Trends Pharmacol Sci* 2013;34:676-88.

25. Körner M, Waser B, Schonbrunn A, et al. Somatostatin receptor subtype 2A immunohistochemistry using a new monoclonal antibody selects tumors suitable for in vivo somatostatin receptor targeting. *Am J Surg Pathol* 2012;36:242-52.

26. Kaemmerer D, Peter L, Lupp A, et al. Molecular imaging with <sup>68</sup>Ga-SSTR PET/CT and correlation to immunohistochemistry of somatostatin receptors in neuroendocrine tumours. *Eur J Nucl Med Mol Imaging* 2011;38:1659-68.

27. Miederer M, Seidi S, Buck A, et al. Correlation of immunohistopathological expression of somatostatin receptor 2 with standardised uptake values in <sup>68</sup>Ga-DOTATOC PET/CT. *Eur J Nucl Med Mol Imaging* 2009;36:48-52.

28. Reubi JC. Peptide receptors as molecular targets for cancer diagnosis and therapy. *Endocr Rev* 2003;24:389-427.

29. Virgolini I, Gabriel M, Kroiss A, et al. Current knowledge on the sensitivity of the <sup>68</sup>Ga-somatostatin receptor positron emission tomography and the SUVmax somatostatin receptor targeting reference range for management of pancreatic neuroendocrine tumours. *Eur J Nucl Med Mol Imaging* 2016;43:2072-83.

30. Ambrosini V, Campana D, Bodei L, et al. <sup>68</sup>Ga-DOTANOC PET/CT Clinical Impact in Patients with Neuroendocrine Tumors. *J Nucl Med* 2010;51:669-73.

31. Barrio M, Czetnin J, Fanti S, et al. The impact of somatostatin receptor-directed PET/CT on the management of patients with neuroendocrine tumor: a systematic review and meta-analysis. *J Nucl Med* 2017;58:756-61.

32. Mikolajczak M, Maecke H R. Radiopharmaceuticals for somatostatin receptor imaging.

*Nuclear Medicine Review* 2016;19:126-32.

33. Deppen SA, Liu E, Blume JD, et al. Safety and efficacy of <sup>68</sup>Ga-Dotatate PET/CT for diagnosis, staging, and treatment management of neuroendocrine tumors. *J Nucl Med* 2016;57:5:708-14.
34. Gabriel M, Decristoforo C, Kendler D, et al. <sup>68</sup>Ga-DOTA-Tyr3-octreotide PET in neuroendocrine tumors: comparison with somatostatin receptor scintigraphy and CT. *J Nucl Med* 2007;48:508-18.
35. Buchmann I, Henze M, Engelbrecht S, et al. Comparison of <sup>68</sup>Ga-DOTATOC PET and <sup>111</sup>In-DTPAOC (Octreoscan) SPECT in patients with neuroendocrine tumours. *Eur J Nucl Med Mol Imaging* 2007;34:1617-26.
36. Ito T, Jensen R T. Molecular imaging in neuroendocrine tumors: Recent advances, controversies, unresolved issues, and roles in management. *Curr Opin Endocrinol Diabetes Obes* 2017;24:15-24.
37. Sundin A, Arnold R, Baudin E, et al. ENETS Consensus Guidelines for the Standards of Care in Neuroendocrine Tumors: Radiological, Nuclear Medicine & Hybrid Imaging. *Neuroendocrinology* 2017;105:212-44.
38. Hope TA, Bergsland EK, Bozkurt MF, et al., Appropriate use criteria for somatostatin receptor PET imaging in neuroendocrine tumors. *J Nucl Med* 2018;59:66-74.
39. Lococo F, Perotti G, Cardillo G, et al. Multicenter comparison of <sup>18</sup>F-FDG and <sup>68</sup>Ga-DOTA-peptide PET/CT for pulmonary carcinoid. *Clin Nucl Med* 2015;40:e183-e189.
40. Venkitaraman B, Karunanithi S, Kumar A, et al. Role of <sup>68</sup>Ga-DOTATOC PET/CT in initial evaluation of patients with suspected bronchopulmonary carcinoid. *Eur J Nucl Med Mol Imaging* 2014;41:856-64.
41. Menda Y, O'Dorisio TM, Howe JR, et al. Localization of unknown primary site with <sup>68</sup>Ga-DOTATOC PET-CT in patients with metastatic neuroendocrine tumor. *J Nucl Med* 2017;58:1054-57.
42. Haug AR, Assmann G, Rist C, et al. Quantification of immunohistochemical expression of somatostatin receptors in neurocrine tumors using <sup>68</sup>Ga-DOTATATE PET/CT. *Radiologe* 2010;50:349-54.
43. Swarts DR, Rudelius M, Claessen SM, et al. Limited additive value of the Ki-67 proliferative index on patient survival in World Health Organization-classified pulmonary carcinoids. *Histopathology* 2017;70:412-22.
44. Ramirez RA, Beyer DT, Diebold AE, et al. Prognostic Factors in Typical and Atypical Pulmonary Carcinoids. *Ochsner Journal* 2017;17:335-40.
45. Bhatkar D, Utpat K, Basu S, et al. Dual Tracer PET Imaging (<sup>68</sup>Ga-DOTATATE and <sup>18</sup>F-FDG) Features in Pulmonary Carcinoid: Correlation with Tumor Proliferation Index. *Indian J Nucl Med* 2017;32:39-41.
46. Ruf J, Schiefer J, Kropf S, et al. Quantification in <sup>68</sup>Ga-DOTA(0)-Phe(1)-Tyr(3)-Octreotide positron emission tomography/computed tomography: can we be impartial about partial volume effects? *Neuroendocrinology* 2013;97:369-74.
47. Sánchez-Crespo A, Andreo P, Larsson SA. Positron flight in human tissues and its influence on PET image spatial resolution. *Eur J Nucl Med Mol Imaging* 2004;31:44-51.

48. Sánchez-Crespo A, Larsson SA. The influence of photon depth of interaction and non-collinear spread of annihilation photons on PET image spatial resolution. *Eur J Nucl Med Mol Imaging* 2006;33:940-47.
49. Soret M, Bacharach SL, Buvat I. Partial-volume effect in PET tumor imaging. *J Nucl Med* 2007;48:932-45.
50. Sanchez-Crespo A. Comparison of Gallium-68 and Fluorine-18 imaging characteristics in positron emission tomography. *Appl Radiat Isot* 2013;76:55-62.
51. Reynaert H, Rombouts K, Vandermonde A, et al. Expression of somatostatin receptors in normal and cirrhotic human liver and in hepatocellular carcinoma. *Gut* 2004;53:1180-9.
52. Velikyan I, Sundin A, Sörensen J, et al. Quantitative and qualitative intrapatient comparison of <sup>68</sup>Ga-DOTATOC and <sup>68</sup>Ga-DOTATATE: NET uptake rate for accurate quantification. *J Nucl Med* 2014;55:204-10.
53. Ilan E, Velikyan I, Sandström S, et al. Tumor-to-blood ratio for assessment of somatostatin receptor density in neuroendocrine tumors using <sup>68</sup>Ga-DOTATOC and <sup>68</sup>Ga-DOTATATE. *J Nucl Med* 2019. [http://doi: 10.2967/jnumed.119.228072](http://doi.org/10.2967/jnumed.119.228072) [Epub ahead of print].
54. Velikyan I, Sundin A, Eriksson B, et al. In vivo binding of [<sup>68</sup>Ga]-DOTATOC to somatostatin receptors in neuroendocrine tumours – impact of peptide mass. *NuclMed Biol* 2010;37:265-75.
55. Uhlén N, Grundberg O, Jacobsson H, et al. <sup>18</sup>F-FDG PET/CT diagnosis of bronchopulmonary carcinoids versus pulmonary hamartomas. *Clin Nucl Med* 2016;41:263-67.
56. Nettelbladt OS, Sundin AE, Valind SO, et al. Combined Fluorine-18-FDG and Carbon-11-Methionine PET for diagnosis of tumors in lung and mediastinum. *J Nucl Med* 1998;39:640-7.
57. Travis WD, Brambilla E, Muller-Hermelink HK, et al. Pathology and genetics of the lung, pleura, thymus and heart. In: World Health Organisation classification of tumours. Lyon, France: IARC Press; 2004:59-61.
58. Aberle DR, Adams AM, Berg CD, et al. Reduced lung cancer mortality with low-dose computed tomographic screening. *N Engl J Med* 2011;365:395-409.
59. Bergman B, Henriksson R. Lungcancer. In: Ringborg U, Dalianis T, Henriksson R, editors. *Onkologi*. 2nd ed. Stockholm: Liber; 2008:339-53.
60. Moore W, Freiberg E, Bishawi M, et al. FDG-PET imaging in patients with pulmonary carcinoid tumor. *Clin Nucl Med* 2013;38:501-05.
61. Stefani A, Franceschetto A, Nesci J, et al. Integrated FDG-PET/CT imaging is useful in the approach to carcinoid tumors of the lung. *J Cardiothorac Surg* 2013;8:223-29.
62. Rindi G, Klimstra DS, Abedi-Ardekani B, et al. A common classification framework for neuroendocrine neoplasms: an International Agency for Research on Cancer (IARC) and World Health Organization (WHO) expert consensus proposal. *Mod Pathol* 2018;31:1770-86.
63. Pelosi G, Sonzogni A, Harari S, et al. Classification of pulmonary neuroendocrine tumors: new insights. *Transl Lung Cancer Res* 2017;6:513-29.
64. Hendifar AE, Marchevsky AM, Tuli R. Neuroendocrine Tumors of the Lung: Current

Challenges and Advances in the Diagnosis and Management of Well-Differentiated Disease. *J Thorac Oncol* 2017;12:425-36.

65. Chan DL, Clarke SJ, Diakos CI, et al. Prognostic and predictive biomarkers in neuroendocrine tumours. *Crit Rev Oncol Hematol* 2017;113:268–82.
66. Walts AE, Ines D, Marchevsky AM. Limited role of Ki-67 proliferative index in predicting overall short-term survival in patients with typical and atypical pulmonary carcinoid tumors. *Mod Pathol* 2012;25:1258-64.
67. Martin B, Paesmans M, Mascaux C, et al. Ki-67 expression and patients survival in lung cancer: systematic review of the literature with meta-analysis. *Br J Cancer* 2004;91:2018-25.
68. Pelosi G, Massa F, Gatti G, et al. Ki-67 Evaluation for Clinical Decision in Metastatic Lung Carcinoids: A Proof of Concept. *Clin Pathol* 2019;12:1-6.
69. Kayani I, Conry BG, Groves AM, et al. A Comparison of <sup>68</sup>Ga-DOTATATE and <sup>18</sup>F-FDG PET/CT in pulmonary neuroendocrine tumors. *J Nucl Med* 2009;50:1927-32.
70. Pelosi G, Bianchi F, Dama E, et al. Most high-grade neuroendocrine tumours of the lung are likely to secondarily develop from pre-existing carcinoids: innovative findings skipping the current pathogenesis paradigm. *Virchows Arch* 2018;472:567-77.
71. Moris D, Ntanasis-Stathopoulos I, Tsilimigras DI, et al. Insights into novel prognostic and possible predictive biomarkers of lung neuroendocrine tumors. *Cancer Genomics Proteomics* 2017;15:153-63.
72. Wolin EM. Advances in the diagnosis and management of well-differentiated and intermediate-differentiated neuroendocrine tumors of the lung. *Chest* 2017;151:1141-46.
73. Caplin ME, Baudin E, Ferolla P, et al. Pulmonary neuroendocrine (carcinoid) tumors: European Neuroendocrine Tumor Society expert consensus and recommendations for best practice for typical and atypical pulmonary carcinoids. *Ann Oncol* 2015; 26:1604–20.